Assessment of some high-order finite difference schemes on the scalar conservation law with periodical conditions

Alina BOGOI[1], Dragos ISVORANU[1], Sterian DANAILA*,[1]

*Corresponding author
[1]"POLITEHNICA" University of Bucharest, Department of Aerospace Engineering,
Splaiul Independenţei 313, 060042, Bucharest, Romania,
bogoi_alina@yahoo.com, ddisvoranu@gmail.com, sterian.danaila@upb.ro*

DOI: 10.13111/2066-8201.2016.8.4.7

Received: 03 October 2016/ Accepted: 24 October 2016/ Published: December 2016

International Conference of Aerospace Sciences "AEROSPATIAL 2016"
26 - 27 October 2016, Bucharest, Romania, (held at INCAS, B-dul Iuliu Maniu 220, sector 6)
Section 1 – Aerodynamics

Abstract: *Supersonic/hypersonic flows with strong shocks need special treatment in Computational Fluid Dynamics (CFD) in order to accurately capture the discontinuity location and his magnitude. To avoid numerical instabilities in the presence of discontinuities, the numerical schemes must generate low dissipation and low dispersion error. Consequently, the algorithms used to calculate the time and space-derivatives, should exhibit a low amplitude and phase error. This paper focuses on the comparison of the numerical results obtained by simulations with some high resolution numerical schemes applied on linear and non-linear one-dimensional conservation low. The analytical solutions are provided for all benchmark tests considering smooth periodical conditions. All the schemes converge to the proper weak solution for linear flux and smooth initial conditions. However, when the flux is non-linear, the discontinuities may develop from smooth initial conditions and the shock must be correctly captured. All the schemes accurately identify the shock position, with the price of the numerical oscillation in the vicinity of the sudden variation. We believe that the identification of this pure numerical behavior, without physical relevance, in 1D case is extremely useful to avoid problems related to the stability and convergence of the solution in the general 3D case.*

Key Words: *Conservative law, Riemann problem, compact numerical schemes, Runge-Kutta schemes*

1. INTRODUCTION

It is a well known fact that numerical simulations, especially DNS and LES, require high resolution discretization techniques in both space and time domains. One major purpose in applying these techniques is the constant pursuit for reducing the numerical dispersion and diffusion bellow the dispersion and diffusion inherent to the physical phenomenon modeled by the numerical scheme. On the other hand, the increased the order of accuracy necessitates enlarging the numerical stencil which leads to a larger computational effort. Another drawback of the high order schemes is associated with the unphysical oscillations generated in the vicinity of discontinuities (shock waves or shear flows). Hence, a thorough analysis of the accuracy of various numerical schemes is required to pinpoint the behavior of these

techniques in the presence of flow discontinuities. In the present paper, we suggest a series of test cases for which the exact analytical solution has been produced and could serve as a better ground for accuracy prediction of the tested high order numerical schemes. For the calculation of the space derivatives, high-order spatial discretization schemes have gained considerable interests in computational acoustics, among them the explicit dispersion relation preserving (DRP) [2], [12] or compact schemes [1],[3-8]. Time integration in CFD is usually done with higher-order Runge-Kutta schemes. In order to improve the dissipation and dispersion characteristics of these schemes, several other schemes were proposed [12], [13]. In many applications, popular time advancing schemes are the classical 3rd- and 4th-order Runge-Kutta schemes because they provide relatively large stability limits. However, for acoustic calculations the stability consideration alone is not sufficient [13], since the Runge-Kutta schemes distribute both dissipation and dispersion errors. Traditionally, the coefficients of the Runge-Kutta schemes are chosen such that the maximum possible order of accuracy is obtained for a given number of stages. It is possible to choose the coefficients of the Runge-Kutta schemes so as to minimize the dissipation and dispersion errors for the propagating waves, rather than to obtain the maximum possible formal order of accuracy. The optimized schemes will be referred to as Low-Dissipation and Dispersion Runge-Kutta (LDDRK) schemes.

In the first part of this paper, the basic concepts of the numerical schemes for space and time integration are discussed and different numerical schemes are used for solving the one-dimensional problem for the convective wave equation and the conservative equation. A comparison between the different methods and different initial conditions is performed in the last part of this paper.

Let us consider the one-dimensional scalar conservative equation:

$$\frac{\partial U(x,t)}{\partial t}+\frac{\partial f[U(x,t)]}{\partial x}=0, \tag{1}$$

where $U(x,t)$ is a conserved quantity and $f(U(x,t))$ describes its flux and (x,t) denotes space and time, respectively. The numerical solution is obtained by discretizing the equation in space and time to obtain the finite difference or finite volume formulation, respectively. Discretizing the differential form of the conservation law in space, we get the semi-discrete equation as

$$\frac{dU_j}{dt}+\left.\frac{\partial f}{\partial x}\right|_{x=x_j}=0,\ \frac{dU_j}{dt}+\frac{\hat{f}_{j+1/2}-\hat{f}_{j-1/2}}{\Delta x}=0, \tag{2}$$

where $U_j=U(x_j,t)$, $x_j=j\Delta x$, $j=\overline{0,N}$ and the term $\hat{f}_{j+1/2}$ is the numerical flux at the edge of each cell $I_j=[x_{j-1/2},x_{j+1/2}]$ that must satisfy the consistency requirement: $\hat{f}_{j+1/2}=\hat{f}(u_{j-r},...,u_{j+s})$, $\hat{f}(u,...,u)=f(u)$. The numerical flux function $\hat{f}(x)$ is required to satisfy exactly

$$f_x\big|_{x=x_j}=[\hat{f}(x_{j+1/2},t)-\hat{f}(x_{j-1/2},t)]/\Delta x,\ f(x)=\frac{1}{\Delta x}\int_{x-\Delta x/2}^{x+\Delta x/2}\hat{f}(\xi)d\xi. \tag{3}$$

The solution of the conservative finite difference formulation of eq. (1), written in the semi-discrete eq. (2), consists of two steps: spatial discretization and time marching.

2. SPATIAL DISCRETIZATION

There are two main classes of high-order accuracy finite difference schemes: explicit schemes and compact or implicit schemes. One of the important differences between the two schemes is that the explicit schemes employ large computational stencils for a given level of accuracy, while implicit schemes use less stencil points and have less dispersion errors compared to explicit schemes of same order of accuracy. In this context, a scheme is regarded as high-order if it has a formal spatial (and temporal accuracy also) higher than three. In the frame of spatial discretization, we are interested in the reconstruction step that computes the solution at the interfaces from the cell-centered solution to the desired order of accuracy. The Padé type scheme approximates the derivatives implicitly from the use of the Taylor series and a tri-diagonal system must be solved. If we consider the general form of a compact scheme with a general order of accuracy $O(\Delta x^r)$ we get

$$\alpha u'_{i-1} + \beta u'_i + \gamma u'_{i+1} = \sum_{j=-4}^{4} a_{i+j} u_{i+j} / \Delta x \quad . \tag{4}$$

A reminder of the coefficients of the classical Padé schemes is presented in Table 1.

Table 1 – Coefficients of numerical schemes for evaluating

Scheme	Padé			Zhong		
	Pade6	Pade8	Pade10	5-2-3-1	7-3-3-1	9-4-1-0
Order *r*	6	8	10	5	7	7
α	1/3	3/8	2/5	25	45	0
β	1	1	1	60	60	60
γ	1/3	3/8	2/5	15	0	0
a_{i-4}	0	0	-1/4200	0	0	15/56
a_{i-3}	0	1/480	1/210	0	1/2	-19/7
a_{i-2}	-1/36	-1/20	-1/15	-5/2	-9	27/2
a_{i-1}	-14/36	-75/96	-39/50	-160/3	-285/4	-51
a_i	0	0	0	15	60	15/4
a_{i+1}	14/36	75/96	39/50	40	45/2	45
a_{i+2}	1/36	1/20	1/15	5/6	-3	-21/2
a_{i+3}	0	-1/480	-1/210	0	1/4	13/7
a_{i+4}	0	0	1/4200	0	0	-9/56

The spatial resolution of the numerical scheme is dictated by the sound waves with the shortest wavelengths and a minimum number of grid-points per wavelength is required. The development of finite difference algorithms that give an adequate solution for this important issue was first proposed in 1992 by Lele [1] who showed the spectral-like resolution of the compact schemes for the evaluation of spatial derivatives.

The idea was not only to increase the order of accuracy but also to expand the range of wavenumbers. This relates to considering the dissipation and dispersion errors of numerical schemes in the framework of Fourier analysis. These schemes called Dispersion-Relation-Preserving (DRP) schemes seek the best compromise between accuracy and resolution producing the most potentially efficient schemes. Following the work of Tam et al. [2] and Kim et al. [3], a series of high-order optimized compact schemes are derived by Zhu et al. [4]. The schemes are written in a general form:

$$\Delta x(\alpha u'_{i-1} + u'_i + \alpha u'_{i+1}) = a(u_{i+1} - u_{i-1}) + b(u_{i+2} - u_{i-2}) + c(u_{i+3} - u_{i-3}) + d(u_{i+4} - u_{i-4}) \qquad (5)$$

and the coefficients are provided in Table 2.

Most high-order central finite-difference schemes can be used for the viscous flux terms and introduce only phase errors but no dissipative errors in the numerical solutions.

The drawback of central schemes is that they are not robust enough for convection dominated flow simulations.

Extra filtering procedures are needed in order to stabilize the computations and control the aliasing errors, which are equivalent to adding numerical dissipation in an ad- hoc manner.

Table 2 – Coefficients of DRP numerical schemes[4] for evaluating u'_i.

	Order 6	Order 8	Order 10
α	0.4111403764203249	0.4278627893013504	0.4388871532438393
a	0.7842616980350271	0.7786068605349324	0.7748150462341548
b	0.0692748674241733	0.0852418595342336	0.0962949739000680
c	-0.0038903521543495	-0.0077472036156208	-0.0110116258189503
d	0	0.0005034551362033	0.0012257054792086
e	0	0	-0.0000771570500869

Taking into account these facts, Zhong [5] obtained a family of finite-difference high-order upwind compact and explicit schemes for the discretization of convective terms for the direct numerical simulations of hypersonic flows with strong shocks. The upwind schemes are determined such that the order of the schemes is one order lower than the maximum achievable order for the central stencil and, as a result, the coefficient of the leading truncation comes as a free parameter to be set.

We have selected only three schemes: a fifth-order upwind compact scheme, Zhong 5-2-3-1, a seventh-order upwind compact inner scheme, denoted Zhong-7-3-3-1 and a seventh-order upwind explicit scheme, Zhong-9-4-1-0. The coefficients are presented in Table 1.

Another family of numerical schemes considered is a combination of cell-node and cell centered compact schemes for the evaluation of $u_{i+1/2}$. We have considered the sixth order compact interpolation scheme given by Lele [1], then three compact schemes of sixth, eighth and tenth order deduced by Zhang [6], the explicit fifth order upstream difference scheme, the fifth-order upwind compact scheme given by Pirozzoli [7] and the 5th-order upwind compact bi-diagonal scheme given by Fu [8]. The general form is the following

$$\Delta x(\alpha u'_{i-1/2-k/2} + \beta u'_{i+1/2-k/2} + \gamma u'_{i+3/2-k/2}) = \sum_{j=-4}^{4} a_{i+j/2} u_{i+j/2} \quad , \qquad (6)$$

where the coefficients are displayed in Table 3.

As the compact interpolation introduces errors that could significantly decrease the resolution for high wave numbers, Zhang schemes stored the values at the cell centers as independent computational variables and used the same scheme for computing the updating values on cell nodes to compute the updating values on cell centers, by simply shifting the indices in (8) by 1/2.

3. TEMPORAL DISCRETIZATIONS

The method of lines is a widely used technique for approximating partial differential equations with large systems of ordinary differential equations (ODEs) in time. The

numerical solution of the scalar conservation law is semi-discretized in the spatial domain using a discrete set of points and after the spatial partial derivatives have been replaced with appropriate finite differences in x_j, we get a system of ODEs

$$\frac{d\boldsymbol{u}}{dt} = L\left(\boldsymbol{u}(t)\right), \tag{7}$$

where the he discrete operator is defined in each x_j

$$L(u_j) = -\left[f\left(U\left(x_{j+1/2},t\right)\right) - f\left(U\left(x_{j-1/2},t\right)\right)\right] / \Delta x. \tag{8}$$

Here, we associate the time dependent vector $\boldsymbol{u}(t)$ with each of these spatial points, specifically $u_j(t) = U(x_j,t),\ j = \overline{0,N}$. System (7) can be solved by a wide variety of standard numerical techniques, explicit or implicit, which have been developed over the years for large systems of ordinary differential equations.

Table 3 – Coefficients of numerical schemes for evaluating $u_{i+1/2}$

Scheme	Lele	Fu	Zhang			Pirozzoli	
	Lele6	Fu5	CCS-T6	CCS-T8	CCS-T10	Pirozzoli5E	Pirozzoli5I
Order r	6	5	6	8	10	5	5
k	0	0	1	1	1	0	0
α	1/3	2/3	-1/12	-3/20	-1/5	0	3
β	1	1	1	1	1	1	6
γ	1/3	0	-1/12	-3/20	-1/5	0	1
a_{i-2}	0	0	0	0	-1/420	1/30	0
$a_{i-3/2}$	0	0	0	2/75	32/525	0	0
a_{i-1}	1/36	1/12	17/36	61/100	34/50	-13/60	1/3
$a_{i-1/2}$	0	0	-16/9	-2	-32/15	0	0
a_i	29/36	47/36	0	0	0	47/60	19/3
$a_{i+1/2}$	0	0	16/9	2	32/15	0	0
a_{i+1}	29/36	11/36	-17/18	-61/100	-34/50	27/60	10/3
$a_{i+3/2}$	1/36	0	0	-2/75	-32/525	0	0
a_{i+2}	0	-1/36	0	0	1/420	-1/20	0

The explicit Runge-Kutta (RK) schemes offer the potential for high order with low storage. Hence, especially for acoustics, high order schemes can be optimized to reduce dissipation and dispersion to form what are known as LDDRK schemes. For an explicit low storage p-stage Runge-Kutta scheme which, in general, advances the solution from time t_n to t_{n+1} can be expressed as follows:

$$\boldsymbol{u}^{(0)} = \boldsymbol{u}^n, \tag{9}$$

$$\boldsymbol{u}^{(s)} = \boldsymbol{u}^n + c_s \Delta t L\left(\boldsymbol{u}^{(s-1)}\right),\ s = 1,\ldots,p, \tag{10}$$

$$\boldsymbol{u}^{n+1} = \boldsymbol{u}^{(p)}, \tag{11}$$

where $\boldsymbol{u}^n$ represent the solution at time step t_n.

The time discretization will be implemented using four different classes of high order Runge–Kutta methods. The first class tested is a third-order TVD Runge–Kutta (TVDRK3) developed by Shu and Osher [10].

$$\boldsymbol{u}^{(1)} = \boldsymbol{u}^n + \Delta t L(\boldsymbol{u}^n) \tag{12}$$

$$\boldsymbol{u}^{(2)} = 0.75\boldsymbol{u}^n + 0.25\boldsymbol{u}^{(1)} + \Delta t L(\boldsymbol{u}^{(1)}) \tag{13}$$

$$\boldsymbol{u}^{n+1} = \boldsymbol{u}^n / 3 + 2\boldsymbol{u}^{(2)} / 3 + 2\Delta t L(\boldsymbol{u}^{(2)}) / 3 \tag{14}$$

Another method, although not TVD, is the fourth-order classical Runge–Kutta scheme:

$$\boldsymbol{u}^{(1)} = \boldsymbol{u}^n + 0.5\Delta t L(\boldsymbol{u}^n), \tag{15}$$

$$\boldsymbol{u}^{(2)} = \boldsymbol{u}^n + 0.5\Delta t L(\boldsymbol{u}^{(1)}), \tag{16}$$

$$\boldsymbol{u}^{(3)} = \boldsymbol{u}^n + \Delta t L(\boldsymbol{u}^{(2)}), \tag{17}$$

$$\boldsymbol{u}^{n+1} = [-\boldsymbol{u}^n + \boldsymbol{u}^{(1)} + 2\boldsymbol{u}^{(2)} + \boldsymbol{u}^{(3)}] / 3 + \Delta t L(\boldsymbol{u}^{(3)}) / 6. \tag{18}$$

The third class consists in a group of three schemes: the 4, 5, 6 standard *p*-stage schemes of p^{th}-order (for linear operator L). The coefficients c_s for the standard 4, 5 and 6 stage Runge-Kutta (SRK) are written in Table 4.

Table 4 – Runge-Kutta scheme coefficients

Stages	c_1	c_2	c_3	c_4	c_5	c_6
SRK4		1/2	1/3	1/4	-	-
SRK5	1	1/2	1/3	1/4	1/5	-
SRK6	1	1/2	1/3	1/4	1/5	1/6
LDDRK4-Hu	1	1/2	0.325994	0.25005000	-	-
LDDRK5-Hu	1	1/2	0.333116	0.23717924	0.197707993	-
LDDRK6-Hu	1	1/2	1/3.	1/4.	0.187441200	0.169193539
LDDRK5-BB	1	1/2	0.330500707	0.23826022	0.1815754860	-
LDDRK6-BB	1	1/2	0.331839543	0.24662360	0.1846469670	0.1179799020

Next, we analyzed three optimized time marching schemes from the class of Low Dispersion and Dissipation Runge-Kutta LDDRK5, LDDRK6 (4th-order) and LDDRK4-6 of Hu[13] minimizing the dissipation and dispersion errors for wave propagation. The 4-6 notation signifies a two-step alternating cycle, where a four stage standard SRK4 is used for the odd time step and a six stage LDDRK6-Hu for the even time step in the cycle. The scheme is a fourth-order accurate scheme in time for linear problem and second-order accurate for nonlinear problem. The advantage of the alternating schemes is that, when the two steps are combined, the dispersion and the dissipation errors can be reduced and higher order of accuracy can be maintained.

Accordingly to Hu [13], the optimized 6-stage scheme has a smaller stability limit than the 5-stage scheme. On the other hand, LDDRK6-Hu and LDDRK4-6 are 4th-order accurate whereas the optimized single-step 5-stage scheme is 2nd order. LDDRK4-Hu was tested but the results are not satisfactory.

Finally, we tested two LDDRK method obtained by Bogey and Bailly [12]. They used the same idea of combining the Taylor series expansion method with the Fourier transform

optimization technique as Hu et al. [13] and computed the relative dissipation and the dispersion errors separately obtaining different coefficients LDDRK5-BB, LDDRK6-BB. We mainly used these Runge–Kutta schemes in our numerical tests because even there were tested other numerical time-marching schemes the results were not encouraging to be reported.

4. NUMERICAL SIMULATIONS

In this section we present the results of the testing and comparison campaign for all schemes summarized in the previous sections. The numerical accuracy and stability of the high-order numerical schemes are analyzed by solving the scalar conservation law equation for different conservative fluxes with periodic conditions.

Test A: A linear conservation law: the advection equation

We start from a single scalar equation where we numerically compute the L_1, L_2 and L_∞ errors and the order of accuracy (or convergence rate) of all the schemes.

The norm of each error is computed by comparison with the exact solution at a certain time that will be indicated for each test.

$$\left\|\boldsymbol{u}-\boldsymbol{u}_{exact}\right\|_1=\frac{1}{N}\sum_{i=0}^{N}\left|u_i-u_{exact,i}\right|,\left\|\boldsymbol{u}-\boldsymbol{u}_{exact}\right\|_2=\sqrt{\frac{1}{N}\sum_{i=0}^{N}\left(u_i-u_{exact,i}\right)^2}\,, \tag{19}$$

$$\left\|\boldsymbol{u}-\boldsymbol{u}_{exact}\right\|_\infty=\max_{i=0,N}\left|u_i-u_{exact,i}\right|. \tag{20}$$

Table 5 – Advection equation. Test A1b. $u_0(x)=\sin(2\pi x),\ T=10$

Method	N	L_1 error	L_1 order	L_2 error	L_2 error	L_∞ error	L_∞ error
Pade6	20	2.29E-03	0	1.91E-03	0	1.92E-03	0
	40	4.31E-05	5.731	3.46E-05	5.787	3.52E-05	5.765
	80	9.76E-07	5.465	7.73E-07	5.485	7.76E-07	5.503
	160	2.67E-08	5.194	2.10E-08	5.202	2.10E-08	5.208
	320	8.24E-10	5.017	6.48E-10	5.019	6.48E-10	5.019
DRPO -6	20	1.84E-03	0	1.49E-03	0	1.53E-03	0
	40	3.79E-05	5.6	3.01E-05	5.631	3.04E-05	5.651
	80	9.19E-07	5.364	7.26E-07	5.374	7.28E-07	5.385
	160	2.62E-08	5.134	2.06E-08	5.14	2.06E-08	5.144
	320	7.97E-10	5.037	6.26E-10	5.04	6.26E-10	5.04
Zhang-CCST6	20	8.54E-04	0	6.72E-04	0	6.74E-04	0
	40	2.61E-05	5.032	2.05E-05	5.033	2.03E-05	5.054
	80	8.10E-07	5.011	6.36E-07	5.012	6.35E-07	4.999
	160	2.53E-08	5.003	1.98E-08	5.003	1.98E-08	5.001
	320	8.01E-10	4.978	6.30E-10	4.977	6.29E-10	4.977
Zhong-9-4-1-0	20	3.96E-03	0	3.26E-03	0	3.23E-03	0
	40	4.77E-05	6.378	3.77E-05	6.433	3.76E-05	6.422
	80	9.75E-07	5.611	7.66E-07	5.621	7.65E-07	5.62
	160	2.65E-08	5.199	2.09E-08	5.199	2.09E-08	5.198
	320	8.10E-10	5.034	6.36E-10	5.034	6.36E-10	5.035

The grid was progressively refined from $N = 20$ points to .. points, by multiplying with a factor of 2. The initial CFL (for the grid of 20 points) is 0.1. A low CFL number is chosen to ensure that the errors due to time discretization are significantly lower than those due to space discretization. We study the performance of all the schemes by applying them to the four classical test problems ([5], [11]) considering periodic boundary conditions on $[-1,1]$, the advection velocity $a = 1$ and the final time of simulation is T .

$$u_t + a u_x = 0 \tag{21}$$

In Table 5 are presented the results obtained with Test A1 at the final simulation time $T = 10$ for the first five best schemes. Given an initial periodical condition $u(x,0) = u_0(x)$, the exact solution at any time for smooth data is given by $u(x,t) = u_0(x - at)$.

Test A1. This test is made to check the convergence rate at large times. Integration times are $T = 1$ and $T = 10$.

$$u_0(x) = \sin(\omega \pi x),\ \omega = 2 \tag{22}$$

Table 6 – Advection equation. Test A1a. $u_0(x) = \sin(2\pi x)$, $T = 1$

Method	N	L_1 error	L_1 order	L_2 error	L_2 order	L_∞ error	L_∞ order
Pade6	20	2.29E-03	0	1.91E-03	0	1.92E-03	0
	40	4.31E-05	5.731	3.46E-05	5.787	3.52E-05	5.765
	80	9.76E-07	5.465	7.73E-07	5.485	7.76E-07	5.503
	160	2.67E-08	5.194	2.10E-08	5.202	2.10E-08	5.208
	320	8.24E-10	5.017	6.48E-10	5.019	6.48E-10	5.019
DRPO -6	20	1.84E-04	0	1.49E-04	0	1.53E-04	0
	40	3.78E-06	5.601	3.01E-06	5.632	3.04E-06	5.652
	80	9.19E-08	5.364	7.26E-08	5.374	7.28E-08	5.384
	160	2.62E-09	5.135	2.06E-09	5.141	2.06E-09	5.144
	320	8.04E-11	5.023	6.32E-11	5.025	6.32E-11	5.025
Zhang-CCS-T6	20	8.54E-05	0	6.72E-05	0	6.74E-05	0
	40	2.61E-06	5.034	2.05E-06	5.035	2.03E-06	5.056
	80	8.10E-08	5.009	6.36E-08	5.01	6.35E-08	4.998
	160	2.53E-09	5.003	1.98E-09	5.003	1.98E-09	5
	320	7.96E-11	4.987	6.26E-11	4.987	6.25E-11	4.987
Zhong-9-4-1-0	20	3.96E-03	0	3.26E-03	0	3.23E-03	0
	40	4.77E-05	6.378	3.77E-05	6.433	3.76E-05	6.422
	80	9.75E-07	5.611	7.66E-07	5.621	7.65E-07	5.62
	160	2.65E-08	5.199	2.09E-08	5.199	2.09E-08	5.198
	320	8.10E-10	5.034	6.36E-10	5.034	6.36E-10	5.035

In Table 6, the used criteria was to select the scheme that gives similar result but with low computational cost from different families of schemes. For example, we choose the 6-th order Padé scheme, because from the 8-th and 10-th order Padé scheme we get the similar

order of accuracy but with larger stencils. In case of Zhong's family it can be seen that we select to present the explicit 9-4-1-0 Zhong's scheme despite the 7-3-3-1 scheme even the accuracy is bigger with an order of magnitude but the effort of calculation is much decreased.

The same reasons generate the choices for the rest of the schemes. As a general consideration, the expected formal order of accuracy described in the next tables is given by the expression

$$n_i = \log_2(L_i^N / L_i^{2N}) \tag{23}$$

where the index successively takes the values $i = 1, 2, \infty$.

The initial CFL is reduced by a factor of $2 / 2^{5/3}$ at each refinement (since the spatial interpolation is fifth order and time marching is third order, this ensures that time discretization errors converge at the same rate as the space discretization ones). The errors due to time discretization are significantly lower than those due to space discretization and therefore all the simulations were ruled by TVDRK3.

Table 7 – Advection equation. Test A2. $u_0(x) = \sin^4(\pi x), T = 1$

Method	N	L_1 error	L_1 order	L_2 error	L_2 order	L_∞ error	L_∞ order
Pade6	20	4.43E-03	0	3.56E-03	0	3.51E-03	0
	40	6.07E-05	6.19	4.83E-05	6.203	4.87E-05	6.175
	80	9.40E-07	6.012	7.38E-07	6.032	7.69E-07	5.984
	160	1.52E-08	5.951	1.20E-08	5.946	1.29E-08	5.893
	320	2.74E-10	5.791	2.17E-10	5.786	2.45E-10	5.721
DRPO -6	20	2.29E-03	0	1.83E-03	0	1.85E-03	0
	40	4.43E-05	5.694	3.50E-05	5.708	3.58E-05	5.688
	80	7.36E-07	5.911	5.80E-07	5.917	6.12E-07	5.87
	160	1.24E-08	5.892	9.79E-09	5.888	1.07E-08	5.836
	320	2.39E-10	5.699	1.89E-10	5.694	2.17E-10	5.626
Zhang-CCST6	20	4.05E-04	0	3.22E-04	0	3.52E-04	0
	40	8.38E-06	5.594	6.75E-06	5.576	7.43E-06	5.565
	80	1.96E-07	5.414	1.57E-07	5.43	1.85E-07	5.328
	160	5.38E-09	5.191	4.30E-09	5.186	5.18E-09	5.157
	320	1.62E-10	5.053	1.29E-10	5.055	1.57E-10	5.043
Zhong-9-4-1-0	20	1.33E-02	0	1.06E-02	0	1.08E-02	0
	40	9.28E-05	7.166	7.40E-05	7.165	7.55E-05	7.16
	80	7.32E-07	6.986	5.79E-07	6.997	6.19E-07	6.929
	160	9.27E-09	6.303	7.34E-09	6.302	8.34E-09	6.215
	320	1.92E-10	5.592	1.53E-10	5.587	1.82E-10	5.521

Test A2. This test is performed to locate possible deteriorations of accuracy due to strong oscillations in the parameters that determine the stencil.

Moreover, this wave is more complex because it has critical points of third degree: $u_0(x_{cr}) = u_0'(x_{cr}) = u_0''(x_{cr}) = 0,\ u_0'''(x_{cr}) \neq 0$

$$u_0(x) = \sin^4(\omega \pi x),\ \omega = 1, T = 1, \tag{24}$$

In Table 7 it should be noted that the hierarchy between numerical schemes is maintained.

We can remark a good convergence for Zhang-CCST6 even for a coarser grid.

Test A3. This test is performed to detect possible decrease in accuracy, due to non-linear argument in the trigonometric function, of the schemes:

$$u_0(x)=\sin\left(\pi x-\sin(\pi x)/\pi\right),\ T=1. \tag{25}$$

In Table 8 it should be noted that the hierarchy between numerical schemes is also maintained.

We can remark a good convergence for Zhang-CCST6 even for a coarser grid.

Table 8 – Advection equation. Test A3. $u_0(x)=\sin\left(\pi x-\sin(\pi x)/\pi\right),\ T=1$.

Method	N	L_1 error	L_1 order	L_2 error	L_2 order	L_∞ error	L_∞ order
Padé classic	20	5.92E-05	0	5.75E-05	0	9.83E-05	0
	40	9.05E-07	6.032	8.97E-07	6.002	1.45E-06	6.082
	80	1.70E-08	5.733	1.70E-08	5.719	2.77E-08	5.713
	160	4.30E-10	5.307	4.09E-10	5.382	6.61E-10	5.388
	320	1.28E-11	5.071	1.19E-11	5.104	1.85E-11	5.156
DRPO -6	20	4.07E-05	0	3.89E-05	0	6.27E-05	0
	40	7.26E-07	5.811	7.27E-07	5.741	1.15E-06	5.764
	80	1.54E-08	5.559	1.52E-08	5.58	2.49E-08	5.537
	160	4.18E-10	5.201	3.91E-10	5.281	6.22E-10	5.321
	320	1.27E-11	5.037	1.18E-11	5.055	1.77E-11	5.133
Zhang-CCST6	20	1.38E-05	0	1.29E-05	0	1.97E-05	0
	40	4.14E-07	5.057	3.78E-07	5.09	5.77E-07	5.094
	80	1.28E-08	5.016	1.16E-08	5.031	1.70E-08	5.089
	160	3.99E-10	5.004	3.59E-10	5.009	5.15E-10	5.042
	320	1.26E-11	4.987	1.15E-11	4.965	1.66E-11	4.954
Zhong-9-4-1-0	20	1.33E-04	0	1.33E-04	0	1.97E-04	0
	40	1.01E-06	7.035	1.06E-06	6.966	1.80E-06	6.777
	80	1.60E-08	5.979	1.55E-08	6.092	2.50E-08	6.171
	160	4.21E-10	5.251	3.87E-10	5.329	5.64E-10	5.469
	320	1.27E-11	5.046	1.17E-11	5.046	1.68E-11	5.067

Test A4. This test is implemented to present the resolution properties of the schemes and the period of integration is $T=8$. The initial condition contains a smooth combination of a Gaussian, a triangle, a square-wave and a half-ellipse, given by

$$u_0(x)=\begin{cases}\left[G(x,z-\delta)+G(x,z+\delta)+4G(x,z)\right]/6, & x\in[-0.8,-0.6]\\ 1, & x\in[-0.4,-0.2]\\ 1-\left|10(x-0.1)\right|, & x\in[0,0.2]\\ \left[F(x,a-\delta)+F(x,a+\delta)+4F(x,a)\right]/6, & x\in[0.4,0.6]\\ 0, & \text{otherwise}\end{cases} \tag{26}$$

where

$$G(x,z)=e^{-\beta(x-z)^2},\ F(x,a)=[\max(1-\alpha^2(x-a)^2,0)]^{1/2} \tag{27}$$

and the constants are taken as $a = 0.5$, $z = -0.7$, $\delta = 0.005$, $\alpha = 10$, $\beta = (\log 2)/36\delta^2$.

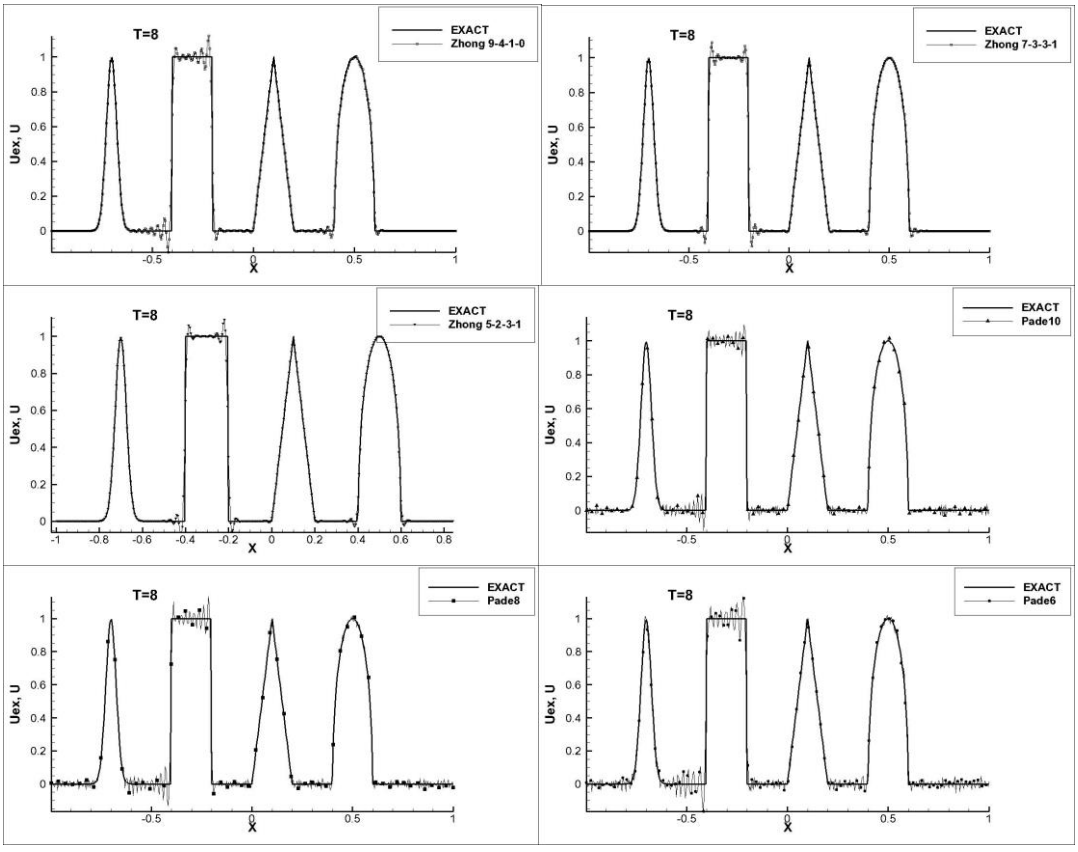

Fig. 1a Comparison of Zhong's and Pade schemes for Test A4

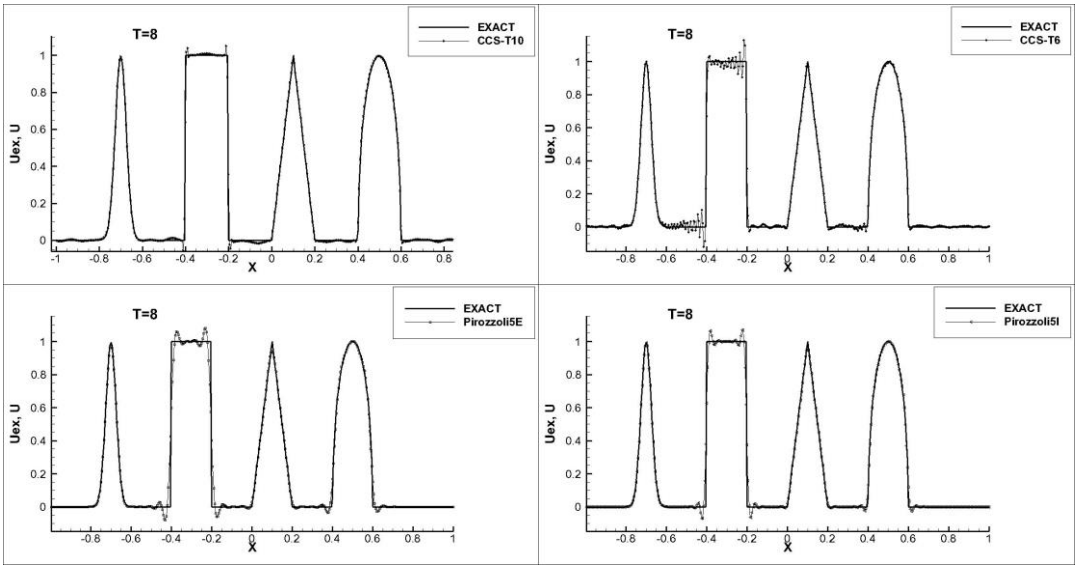

Fig. 1b Comparison of Zhang's and Pirozzoli schemes for Test A4

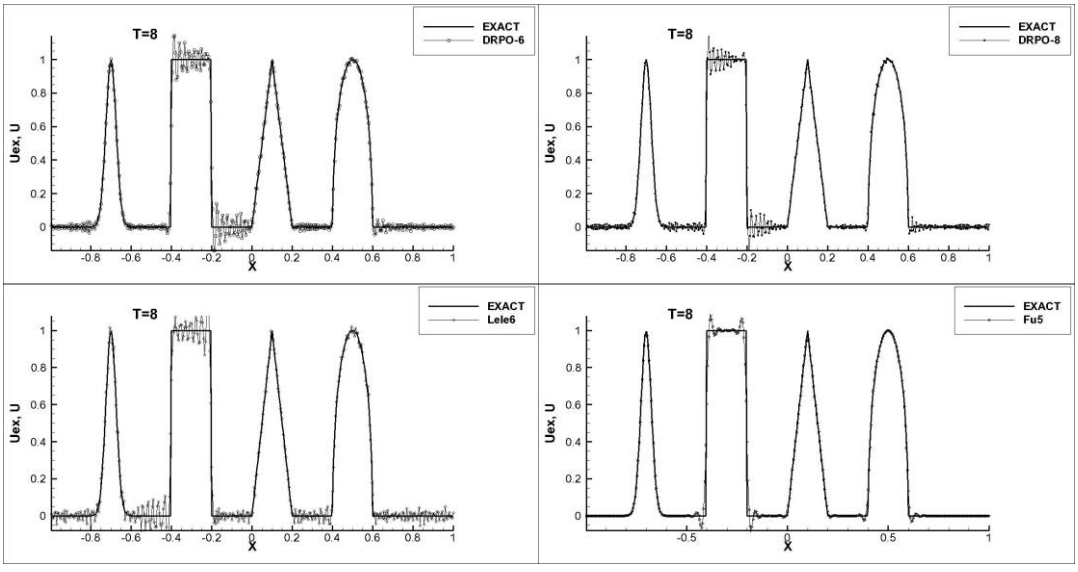

Fig. 1c Comparison of Tam, Lele and Fu schemes for Test A4

Thus, the Gaussian and the ellipse wave are best represented by Zhong 5-2-3-1, Fu5 and Pirozzoli5I.The results at $T=8$ with 400 grid intervals are shown in Figs. 1-5. It can be seen that the schemes selected above resolve different the geometrical shapes.

The triangle wave is more accurately represented by CCS-T10 and Zhong 9-4-1-0. The square waves are not precisely represented by any method, except on CCS-T10.

Nevertheless, one observes many spurious oscillations in all the solution given by the numerical methods.

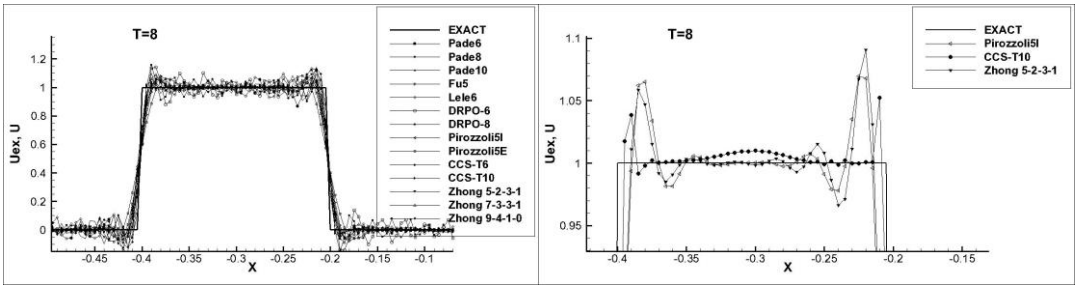

Fig. 2 Detailed Square. Comparison of schemes of for Test 4

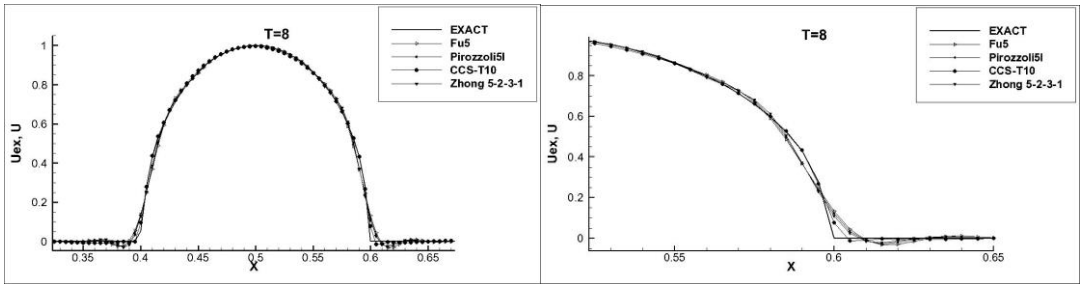

Fig. 3 Detailed Ellipse .Comparison of schemes of for Test 4

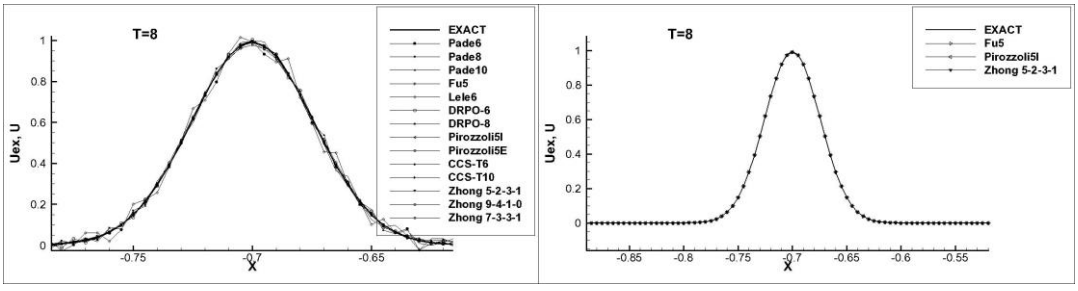

Fig. 4 Detailed Gauss pulse. Comparison of schemes for Test 4

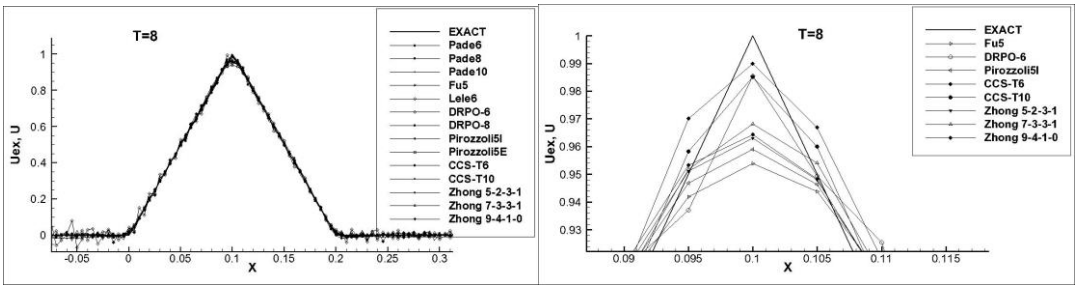

Fig. 5 Detailed triangles. Comparison of schemes for Test 4

Test B: The inviscid Burgers equation

The inviscid Burgers equation is an example of equation with non-linear convex flux, $f(u)=u^2/2$. The problem is solved subject to initial condition

$$u(x,0)=1+0.5\sin(\pi x) \tag{28}$$

and considering periodic boundary conditions on $[-1,1]$, $u(-1,t)=u(1,t)$ [9]. The non-linearity of the conservation equation implies that discontinuities may develop even from smooth initial conditions. The problem provides an initial solution which is smooth and this allows for accuracy and order of convergence analyses. After a certain time $T_s=-1/\min[f''(u(x,0))]_{x\in[-1,1]}$, a shock is developed in the solution[14], [15]. The exact solution, prior to shock formation, is defined implicitly as

$$u(x,t)=1+0.5\sin\left[\pi\left(x-u(x,t)t\right)\right] \tag{29}$$

Table 9: Burgers equation. Test B1a. $u_0(x)=1+0.5\sin(\pi x)$, $T=0.5$, $N=80$

Method	L_1 error	L_2 error	L_∞ error
Pirozzoli5E	2.55E-04	7.02E-04	2.85E-03
Pirozzoli5I	8.24E-05	2.04E-04	7.43E-04
Lele6	1.03E-04	2.14E-04	8.40E-04
DRPO-6	7.19E-05	1.18E-04	3.84E-04
Pade6	1.03E-04	2.14E-04	8.40E-04
Zhong 5-2-3-1	7.33E-05	1.69E-04	7.16E-04
Zhang-CCS T6	4.53E-05	9.08E-05	3.50E-04
Zhong 9-4-1-0	4.33E-05	8.46E-05	2.80E-04

An iterative procedure like Newton-Raphson was used to compute the exact solution up to the shock develops. As the shock time is $T_s=2/\pi$, we consider two final simulation times, before and after the shock: $T=0.5$ and $T=1.0$ at a $CFL=0.5$. Table 9 shows the

results at $T=0.5$ with the grid number of $N=80$ and Table 10 with the grid number $N=400$ considering $CFL=max(u_i)dt/dx$ and just eight representative numerical schemes. For these cases, there is indistinguishable difference between all the schemes tested in this paper.

On the fine grid, all schemes yield comparable errors. In smooth regions the numerical solutions are very accurate in all three norms.

Table 10: Burgers equation. Test B1b., $u_0(x)=1+0.5\sin(\pi x), T=0.5$, $N=400$

Method	L_1 error	L_2 error	L_∞ error
Pirozzoli5E	3.20E-07	9.57E-07	6.04E-06
Pirozzoli5I	1.47E-07	2.87E-07	1.20E-06
Lele6	1.51E-07	2.97E-07	1.19E-06
DRPO-6	1.48E-07	2.95E-07	1.35E-06
Pade6	1.51E-07	2.97E-07	1.19E-06
Zhong 5-2-3-1	1.48E-07	2.87E-07	1.15E-06
Zhang-CCS T6	1.49E-07	2.96E-07	1.27E-06
Zhong 9-4-1-0	1.48E-07	2.87E-07	1.15E-06

The problem provides an initial flow in which the solution is smooth, thus allowing for convergence order of accuracy estimates. After a certain time (the shock develops at $T_s=2/\pi$), a shock forms in the solution and the non-oscillatory nature of the schemes can be assessed. Here $T=0.5$ is used for convergence tests and $T=1.0$ for the shock capturing test. The evolutions of the schemes are illustrated in Fig. 6 for the Burgers equation. The evolution on the left refer to the solution before shock formation, $T=0.5$ and the evolution on the right refer to the solution after shock formation, $T=1.0$. One can notice that the "fine grid solution" is the solution obtained on a grid of 2000 points with Pirozzli5I scheme since the exact solution is not available in analytical form, Fig. 7 (right).

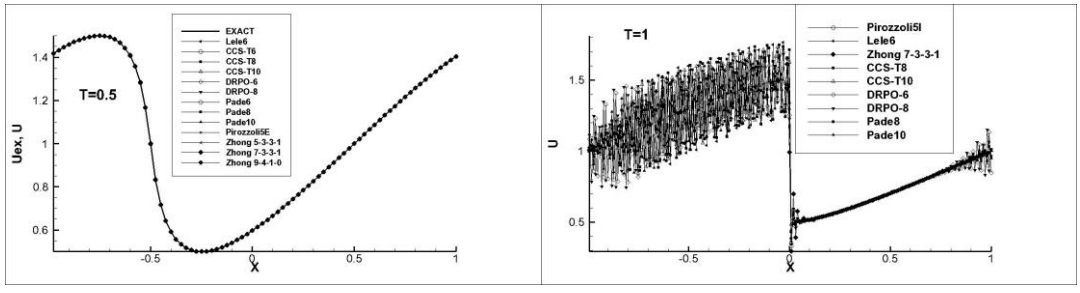

Fig. 6 Solution of Burgers equation at $T=0.5$ and $T=1.0$

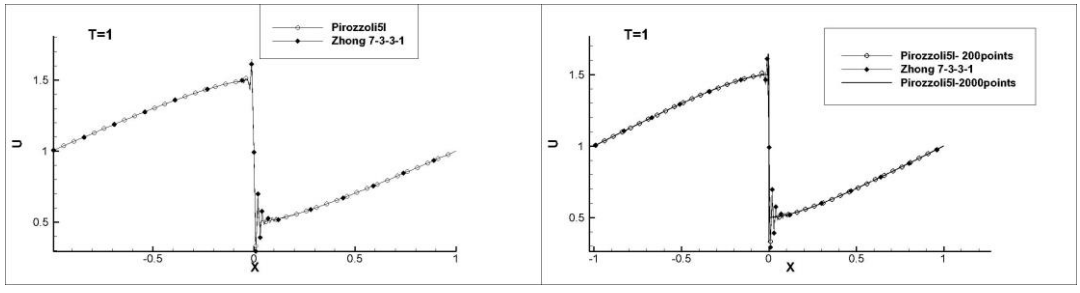

Fig. 7 Solution of Burgers equation for two representative schemes at $T=1.0$

The solutions obtained using Pirozzoli5I and Zhong 7-3-3-1 schemes seem to present some spurious oscillations in the vicinity of the shock for this problem. We do not intend to represent the results for the other schemes due to strong oscillations in accuracy. Regarding all the multistage time discretization R-K schemes, the accurate results were given by LDDRK4-6.

4. CONCLUSIONS

The most known non-compact and compact schemes are analyzed. Their behavior, in terms of accuracy and convergence properties, is studied on the linear advection equation and the inviscid Burgers equation. The schemes are tested on smooth data for periodical conditions. The linear advection equation is the simplest example of a scalar hyperbolic PDE, while the inviscid Burgers equation is an example of a scalar nonlinear hyperbolic PDE. The convergence behavior of the schemes is studied on smooth problems for which the exact solution is known.

This assessment was made because in literature are sometimes presented only the cases which are favorable to a certain method and our purpose is to present objectively the capacity of each methods for simple cases, like scalar conservation law problem. All schemes converge to the proper weak solution for linear flux and smooth initial conditions. However, when the flux is non-linear, the discontinuities may develop from smooth initial conditions and the shock must be correctly captured. All the schemes accurately identify the position of the shock, with the price of the nonrealistic oscillation on the location of the discontinuity. Therefore, a particular care should be given in choosing the numerical methods to be sure that the results are not altered for multidimensional computational fluid dynamics problems.

REFERENCES

[1] S. K. Lele, Compact finite difference schemes with spectral-like resolution, *Journal of Computational Physics*, **103**, 16, 1992.

[2] C. K. W. Tam, J. C. Webb, Dispersion-Relation-Preserving Finite Difference Schemes for Computational Acoustics, *J. Comput. Phys.*, (**107**), 262-281,1993.

[3] J. W. Kim and D. J. Lee, Optimized compact finite difference schemes with maximum resolution, *AIAA J.* **34**, 887-893, 1996.

[4] W. J. Zhu, *Aero-Acoustic Computations of Wind Turbines*, PhD thesis, Technical University of Denmark, September 2007.

[5] X. Zhong, High-order finite-difference schemes for numerical simulations of hypersonic boundary-layer transition, *J. Comp. Phys.* **144**, 662–709, 1998.

[6] X. Liu, S. Zhang, H. Zhang, C-W. Shu, A new class of central compact schemes with spectral-like resolution I: Linear schemes, *J. Comput. Phys*., **248**, 235-256, 2013.

[7] S. Pirozzoli, Conservative hybrid compact-WENO schemes for shock-turbulence interaction, *J Comp Phys*., **178**(1):81–117, 2002.

[8] D. X. Fu, Y. W. Ma, A high order accurate difference scheme for complex flow fields, *J Comput Phys*., **134**: 1–15, 1997.

[9] A. Harten, B. Engquist, S. Osher, S. R. Chakravarthy, Uniformly high order accurate essentially non-oscillatory schemes, III. *J. Comput. Phys. 71*(2), 231–303, 1987.

[10] C.-W. Shu and S. Osher, Efficient implementation of essentially non-oscillatory shock capturing schemes, *J. Comput. Phys.* **77**, 439, 1988.

[11] D. Levy, G. Puppo and G. Russo, Central WENO schemes for hyperbolic systems of conservation laws, *Math. Modelling Numer. Anal.*, Vol. **33**, No 3, p. 547-571, 1999.

[12] C. Bogey, C. Bailly A Family of Low Dispersive and Low Dissipative Explicit Schemes for Computing the Aerodynamic Noise, *AIAA-paper 2002-2509*, 2002.

[13] F. Q. Hu, M. Y. Hussaini and J. L. Manthey, Low-dissipation and low-dispersion Runge-Kutta schemes for computational acoustics, *J Comput Phys*., Vol. **124**, No. 1, pp. 177-191, 1996.
[14] S. Dănăilă, C. Berbente, *Metode numerice în mecanica fluidelor*, Ed. Academiei, 2003.
[15] R. J. LeVeque, *Finite Volume Methods for Hyperbolic Problems*, Cambridge University Press, 2002.